JOURNAL OF GEOPHYSICAL RESEARCH, VOL. 114, C02004, doi:10.1029/2008JC004979, 2009

Trends in primary production in the California Current detected with satellite data

Mati Kahru,[1] Raphael Kudela,[2] Marlenne Manzano-Sarabia,[3] and B. Greg Mitchell[1]

Received 18 June 2008; revised 13 November 2008; accepted 16 December 2008; published 12 February 2009.

[1] Several ocean primary production algorithms using satellite data were evaluated on a large archive of net primary production (NPP) and chlorophyll-a (Chl-a) measurements collected by the California Cooperative Fisheries Investigations program in the California Current. The best algorithm matching in situ data was found by empirically adjusting the Behrenfeld-Falkowski Vertically Generalized Production Model. Satellite-derived time series of NPP were calculated for the California Current area. Significant increase in NPP and Chl-a annual peak levels, i.e., the "bloom magnitude," were found along the coasts of the California Current as well as other major eastern boundary currents for the period of modern ocean color data (1997–2007). The reasons for this increase are not clear but are associated with various environmental conditions.

Citation: Kahru, M., R. Kudela, M. Manzano-Sarabia, and B. G. Mitchell (2009), Trends in primary production in the California Current detected with satellite data, *J. Geophys. Res.*, *114*, C02004, doi:10.1029/2008JC004979.

1. Introduction

[2] Ocean primary production (PP) is a crucial component of the Earth's biogeochemical cycles of carbon and other major chemical elements [*Field et al.*, 1998]. Net primary production (NPP, g C m^{-2} d^{-1}), i.e., total primary production minus the losses due to respiration of the phytoplankton, provides the upper bound for production at higher trophic levels [*Behrenfeld et al.*, 2006]. In situ measurement of PP or NPP is extremely time-consuming and not representative of a larger area because of high spatial and temporal variability. Estimating PP at regional and global scales is therefore difficult without the quasi-synoptic view provided by satellite data or numerical models. Current satellite-based estimates of primary production have achieved limited success and improving those estimates is therefore needed [e.g., *Friedrichs et al.*, 2008]. Here we are primarily interested in applying the best fit model to evaluate temporal trends in NPP and are less concerned with the formulation of the models. However, since there is no clear choice in which NPP model should be applied to regional studies, we begin by evaluating 5 common models, and then use the statistically best model to describe PP trends in the California Current System.

2. PP Models

[3] Many models of depth-integrated NPP applicable to remotely sensed data are available [*Friedrichs et al.*, 2008]. In this work we compare five well-known models. The simplest estimate of NPP is provided by the Eppley Square Root (ESQRT) model [*Eppley et al.*, 1985] that estimates depth-integrated primary production (g C m^{-2} d^{-1}) as the square root of surface chlorophyll-a concentration (Chl-a, mg m^{-3}). This purely empirical relationship represents the baseline of NPP prediction accuracy. If a complicated NPP model does not improve on the accuracy of the simple ESQRT model then it obviously has serious flaws.

[4] The Vertically Generalized Production Model (VGPM) by *Behrenfeld and Falkowski* [1997] is the best known NPP model. VGPM uses satellite estimates of Chl-a, photosynthetically active radiation (PAR) and sea surface temperature (SST) as input. Various authors have proposed modifications to the VGPM, and we include the *Kameda and Ishizaka* [2005] model (KI) that is based on the assumption that both Chl-a and NPP can be partitioned into a stable part because of a small phytoplankton fraction and a variable part because of the large phytoplankton fraction. It also assumes that the chlorophyll-specific productivity is inversely proportional to phytoplankton size.

[5] The *Marra et al.* [2003] model (MARRA) uses the same inputs of Chl-a, PAR and SST but is based on chlorophyll-specific phytoplankton absorption, which is parameterized empirically as a function of SST. Absorption by photosynthetic pigments is distinguished from total absorption; the former is used to calculate productivity and the latter is used to estimate light attenuation in the water column. The depth profile of Chl-a is estimated assuming a Gaussian shape with parameters determined by the surface value.

[6] The Carbon-based Production Model (CbPM) [*Behrenfeld et al.*, 2005] is a new approach to NPP assessment that uses satellite-derived carbon to Chl-a ratio to predict phytoplankton growth rate. It utilizes a semianalytic algorithm to invert satellite-detected radiance into surface

[1]Scripps Institution of Oceanography, University of California, San Diego, La Jolla, California, USA.
[2]Ocean Sciences Department, University of California, Santa Cruz, California, USA.
[3]Centro de Investigaciones Biológicas del Noroeste, La Paz, Baja California Sur, México.

0148-0227/09/2008JC004979$09.00

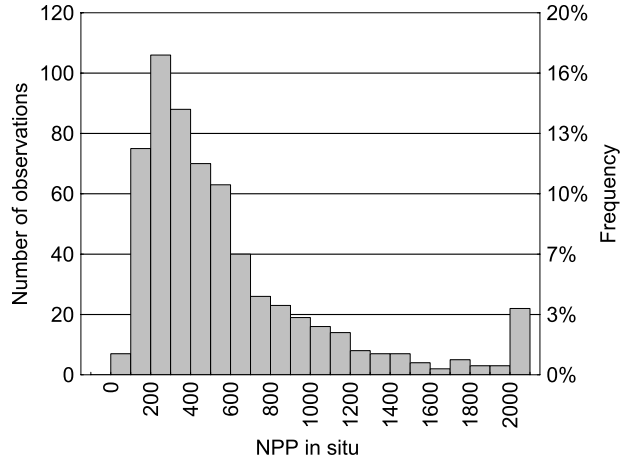

Figure 1. Histogram of in situ CalCOFI NPP measurements (N = 608) that have a corresponding satellite match-up with the VGPM algorithm using Chl-a, PAR, and SST.

Chl-a and particulate backscatter coefficient (b_{bp}, m^{-1}) at 443 nm. The backscatter coefficient is then converted into phytoplankton carbon biomass (C) and NPP is calculated as the product of C and the specific phytoplankton growth rate (d^{-1}). Five input data sets are used, including the coefficient of attenuation of downwelling irradiance at 490 nm (K_{490}, m^{-1}) and the mixed layer depth (MLD, m).

3. Statistics

[7] The skill of the models to estimate NPP was assessed using several statistics. As a first step we used linear regression of $\log_{10}$-transformed variables and calculated the coefficient of determination, r^2. The total root mean square difference (RMSD) summed over $\log_{10}$-transformed data points was used as the total error of the model. RMSD is composed of two components, the bias representing the difference between the means of the two fields, and the centered pattern RMSD ($RMSD_{CP}$, the unbiased RMSD) representing the differences in the variability of the two fields [*Friedrichs et al.*, 2008]. The existence of trends and their significance was detected with the Sen Slope estimator [*Gilbert*, 1987]. Sen slope is a nonparametric estimate of the slope that involves computing slopes for all the pairs of time points and then using the median of these slopes as an estimate of the overall slope. Similar estimates of the slope were obtained with the traditional linear least squares regression but the Sen slope estimator is preferable because of its less sensitivity to outliers.

4. Data

[8] The California Cooperative Fisheries Investigations (CalCOFI) [*Mantyla et al.*, 1995] has been collecting primary production data with the same methodology since January 1984. The half-day, simulated on-deck incubation values of carbon-14, integrated over the euphotic layer, were multiplied by 1.8 to obtain equivalent full day net primary production [*Eppley*, 1992]. The archive has 1862 measurements collected during 1984–2007 covering a wide range of NPP values from oligotrophic offshore waters to productive coastal waters (Figure 1). About 610 of these NPP measurements were collected during the availability of data from SeaWiFS (from September 1997), the primary ocean color sensor used in this study.

[9] The five NPP models were evaluated by comparing CalCOFI primary production values with coincident satellite estimates obtained for the nearest valid day. A 3 × 3 pixel window centered at the nearest satellite pixel was used and NPP estimates were calculated for all valid pixels in that window. The satellite data input was declared valid if at least 3 valid pixels were found in the 3 × 3 pixel window. The data set nearest in time was used. If the nearest day had no valid data then the next nearest day was used. The arithmetic mean NPP of valid pixels in the 3 × 3 pixel window of the nearest valid day was used in the comparison with in situ data.

[10] Daily mapped images of Chl-a, K490, PAR and SST were obtained from the NASA Ocean Color website (data available at http://oceancolor.gsfc.nasa.gov/). The standard OC4v4 Chl-a algorithm [*O'Reilly et al.*, 1998] was used for all but the CbPM model. The 9-km daily Chl-a data from SeaWiFS were used from September 1997 to July 2002 and the merged SeaWiFS-MODIS-Aqua daily Chl-a data from July 2002 to the end of 2007. PAR (Einstein m^{-2} d^{-1}) data were derived from daily SeaWiFS 9-km data sets for the whole period. Sea surface temperature was obtained from the AVHRR Pathfinder (version 5) 8-day composites (data available at http://www.nodc.noaa.gov/sog) until 2002 and from the merged MODIS Terra and MODIS Aqua daytime 8-day SST data after that period. The daily Chl-a and particulate backscattering coefficient ($b_{bp}443$) for the CbPM model were derived using the GSM01 semianalytical algorithm [*Maritorena et al.*, 2002] from SeaWiFS data (1997–2002, version 1.4) and from the merged SeaWiFS-MODIS-Aqua data (2002–2007, version 5.4) and were provided by S. Maritorena. The merged SeaWiFS-MODIS-Aqua data set was preferred to the equivalent single sensor data set as data merging reduces the number of missing pixels due to clouds and orbit coverage. The mixed layer depth data for the CbPM model were obtained from the Ocean Productivity Home Page (data available at http://science.oregonstate.edu/ocean.productivity) and were derived using the Fleet Numerical Meteorology and Oceanography Center model.

5. Evaluation of NPP Models

[11] Scatterplots of satellite estimates of NPP using the ESQRT and VGPM models versus in situ measurements (Figures 2a and 2b) show that while the minimalistic ESQRT model provides a useful correlation based on only surface Chl-a, it explains only 55% of the total $\log_{10}$ variance. The VGPM model improves the fit compared to the baseline ESQRT model but the difference is relatively small (r^2 increased from 0.553 to 0.662, see Table 1). It is obvious that most of the predictive power of the VGPM model derives from the correlation of NPP with Chl-a. The other parameters of the regression (slope, intercept and RMSDcp) are also improved in the VGPM compared to ESQRT model. Although the KI model has an ecologically sound basis and improves the r^2 value compared to ESQRT, it does not provide improvement over the standard VGPM and is even more biased.

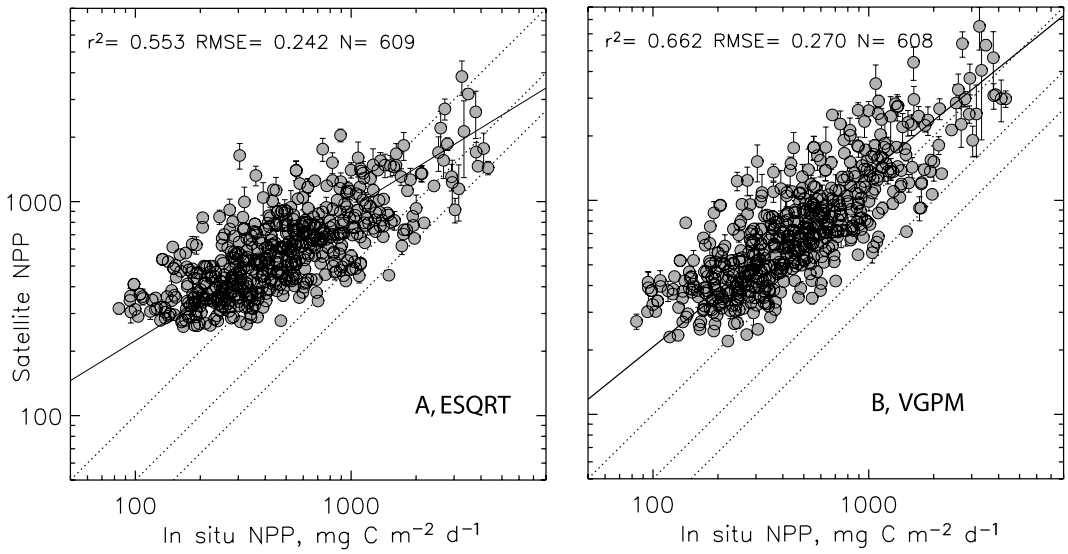

Figure 2. Satellite-estimated NPP versus in situ CalCOFI measurements. The solid black line is the least squares linear regression (in log-log space), and the dotted lines show the one-to-one line, the 1/2, and the 1/3 lines, respectively. The circles are centered at the mean of each 3 × 3 pixel satellite pixel window, and the vertical lines show the 1 standard deviation for the same window. If standard deviation is small, then the vertical line becomes invisible. (a) ESQRT model, (b) VGPM model.

[12] The MARRA model is based on fundamental photophysiology and has good potential to be the basis for the next generation algorithm. It had the least RMSD error and was least biased. However, the scatter was somewhat higher. Because of the higher RMSDcp error and lower r^2 compared to VGPM (RMSDcp 0.207 versus 0.188 of VGPM) it did not represent the best fit to the CalCOFI NPP data.

[13] The CbPM model produced the lowest r^2 and was also more biased than VGPM (Table 1) despite the increased complexity of this model. The r^2 is even lower than that of ESQRT, indicating that some of the assumptions are not applicable to the California Current System. It is likely that part of the poor performance of CbPM is not due to the model itself but due to the errors in its input data sets, e.g., the MLD data and the GSM01 derived b_{bp} and Chl-a. The GSM01 algorithm is more sensitive to atmospheric correction errors and not particularly suitable for coastal applications [*Kudela and Chavez*, 2004]. However, *Kostadinov et al.* [2007] found that GSM01 derived Chl-a estimates have similar accuracy to the standard algorithms.

[14] For all of the model-data comparisons some of the error can be attributed to the time difference between the in situ and satellite measurement. A histogram of this time difference for Chl-a is shown in Figure 3. About two thirds of the NPP estimates had a time difference of their Chl-a estimate of 0 or 1 days. However, some had considerably longer time differences because of cloudy periods. In general, Chl-a concentration does not change drastically during 1–2 days as its decorrelation timescale is approximately 4 days in the region between 200 and 400 km from the coast where most of the CalCOFI measurements are from [*Abbott and Letelier*, 1998]. However, within 200 km of the coast the decorrelation timescales may be shorter. *Abbott and Letelier* [1998] report decorrelation scales of only 2 days for both SST and Chl-a, while *Vander Woude* [2006] reported decorrelation scales ranging from 3–6 days for SST and 1–8 days for Chl-a in central California using both Eulerian and Lagrangian data sets. Thus the time lag

Table 1. Statistics Showing the Success of Various Satellite NPP Algorithms to Estimate in Situ NPP Measurements of the CalCOFI Program

Algorithm	r^2	RMSD	RMSDcp	Slope	Intercept
ESQRT	0.553	0.242	0.220	0.461	1.533
VGPM	0.662	0.269	0.188	0.662	1.091
KI	0.620	0.248	0.210	0.439	1.616
MARRA	0.636	0.216	0.207	0.789	0.503
CbPM	0.389	0.262	0.260	0.537	1.286
VGPM-CAL	0.661	0.188	0.188	1.0	0.0

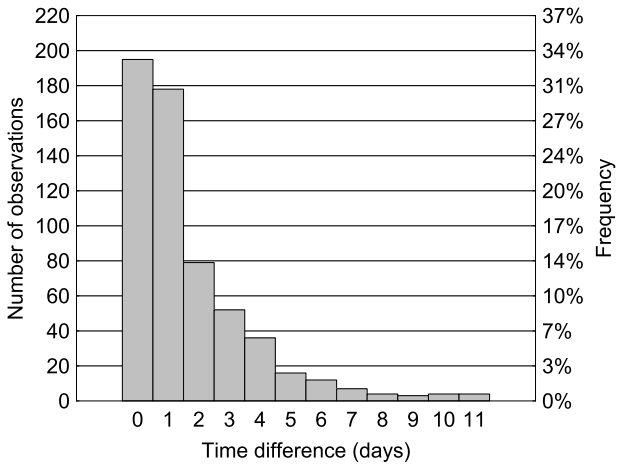

Figure 3. Histogram of the time difference in days in the matching Chl-a value used in the satellite-derived VGPM model.

with satellite data may be significant. As temporal correlation must decrease with increasing time difference we expect that the correlation between satellite and in situ NPP values is lower as the time difference between in situ and satellite Chl-a measurements is higher. However, we actually observed that r^2 was lower for the NPP samples with the same day Chl-a sample compared to the rest of the data set (r^2 is 0.58 for time difference of 0 days and 0.69 for time difference > 0 days) and the difference between r^2 appeared to be significant ($P < 0.05$). The existence of the same day Chl-a estimate (time lag of 0 days) means that the day of NPP sampling was clear whereas a time lag of >1 days means that the sampling day was most likely cloudy. It is therefore possible that the satellite-derived NPP estimates are statistically better matched to in situ productivity measurements during overcast days, despite the time lag.

[15] PAR can be quite variable from day to day (i.e., clear or cloudy) and has a strong effect on in situ NPP measurements. The time difference of the PAR data used in the satellite NPP estimates was only 0 or 1 day because of the SeaWiFS orbit characteristics. Clouds do not interfere in satellite PAR estimates. No influence of the PAR time difference was observed on NPP estimates.

[16] The influence of SST on the VGPM and related models is relatively small. We therefore used 8-day SST estimates instead of daily estimates in order to minimize the number of missing NPP match-ups due to missing concurrent SST data.

[17] In summary, while the MARRA model had the least bias, the VGPM model had the highest r^2 and the lowest unbiased RMSD (Table 1). We therefore decided to use the VGPM model after a linear transformation in order to remove the mean bias. The resulting algorithm, named VGPM-CAL, is calculated as following: VGPM-CAL = $10\text{^}(\text{LOG}_{10}(\text{VGPM})) - 0.1924$. As the mean bias in log-log space is removed, the resulting regression has slope 1.0 and intercept 0.0 while keeping the same r^2 (Table 1).

[18] It has to be noted that even the best algorithm explains only 66% of the total NPP variation. Even after removing the overall mean bias, some residual spatial bias is still present in the NPP estimates. The VGPM-CAL model seems to overestimate in situ NPP in the northwest offshore region and in the northeast coastal upwelling region (not shown).

6. Time Series of NPP

[19] We applied the VGPM-CAL model to monthly satellite data using standard SeaWiFS (1997–2002) and the merged SeaWiFS-Aqua data (2002–2007) for Chl-a, SeaWiFS for PAR and daytime AVHRR Pathfinder version 5 (1997–2002) or the daytime merged MODIS Terra-Aqua data (2002–2007) for SST. In order to extend the time series we used the November 1996 to June 1997 Chl-a data from the Japanese Ocean Color and Temperature Sensor (OCTS) and the corresponding SST data from AVHRR Pathfinder data. The SeaWiFS type PAR data were not available for the OCTS period and we therefore used the mean monthly PAR of the SeaWiFS period as a substitute for the actual monthly PAR.

[20] The annual cycle of monthly NPP in any location has an important characteristic, the annual maximum that is related to the bloom magnitude. The height and timing of the annual maxima are ecologically important in the fate of the newly produced organic matter. We assume that short and high maxima in NPP are more likely to sink out of the euphotic zone (i.e., enhance export production) and cause oxygen deficiency in poorly mixed bottom waters. On the other hand, lower and longer-lasting maxima in NPP are more likely to result in enhanced trophic transfer within the euphotic zone. We base this conclusion on the expected delay between primary production and secondary consumption; a short, large phytoplankton bloom event is likely to sink out of the euphotic zone before maximal secondary production is realized. We recognize that other forms of temporal mismatches between primary production and grazers may also be important [*Wheeler et al.*, 2003]. We suggest that the magnitude of the annual maximum is an important proxy for assessing interannual trends in productivity or biomass. We therefore created a time series of annual maxima in NPP using monthly NPP composites. Figure 4 shows that during the last 11 years (1997–2007) the annual maxima in NPP have increased along the coast of the California Current. A small area off the coast of the Mexican states of Nayarit and Jalisco (around Punta Mita) has experienced a decrease in the annual NPP maximum during this time period. A similar increase in satellite-detected Chl-a has been reported earlier [*Kahru and Mitchell*, 2008]. We acknowledge that these estimates of increase or decrease are based on a relatively short period and are sensitive to the large interannual variability.

7. Discussion

[21] The standard satellite Chl-a algorithm is known to work well in the California Current [*Kahru and Mitchell*, 1999, 2001] with typical r^2 values of about 0.8–0.9 and no significant bias. Previous attempts to validate satellite-derived NPP data with the CalCOFI NPP measurements [*Balch and Byrne*, 1994; *Kahru and Mitchell*, 2002] have found a relatively poor fit with lower r^2 and a large bias. In this work we have empirically adjusted the VGPM satellite algorithm to provide the best fit to the in situ data. This is consistent with earlier efforts based on independent data from the California Current System. *Kudela et al.* [2006] modified VGPM to remove the SST term, achieving a slope of 1.0 and an r^2 value of 0.667 for the Pacific Northwest, while *Chavez et al.* [2002] modified the SST term by applying a seasonally averaged function. The other models, including the recently proposed carbon-based model (CbPM) were less accurate in predicting in situ NPP measured by the CalCOFI program. All except the MARRA model produced significant overestimation at low NPP values. The MARRA model had least bias but its predictive capability was somewhat lower than that of the VGPM. It is clear that some of the errors in the skill of the NPP models are due to the errors in the input fields. The CbPM model depends on more input fields (5 versus 3 for VGPM, KI and MARRA). It also relies on the complex and sensitive GSM01 algorithm for deriving Chl-a and b_{bp} from water-leaving radiances that are determined with significant error, especially near the coast and with complex atmospheric

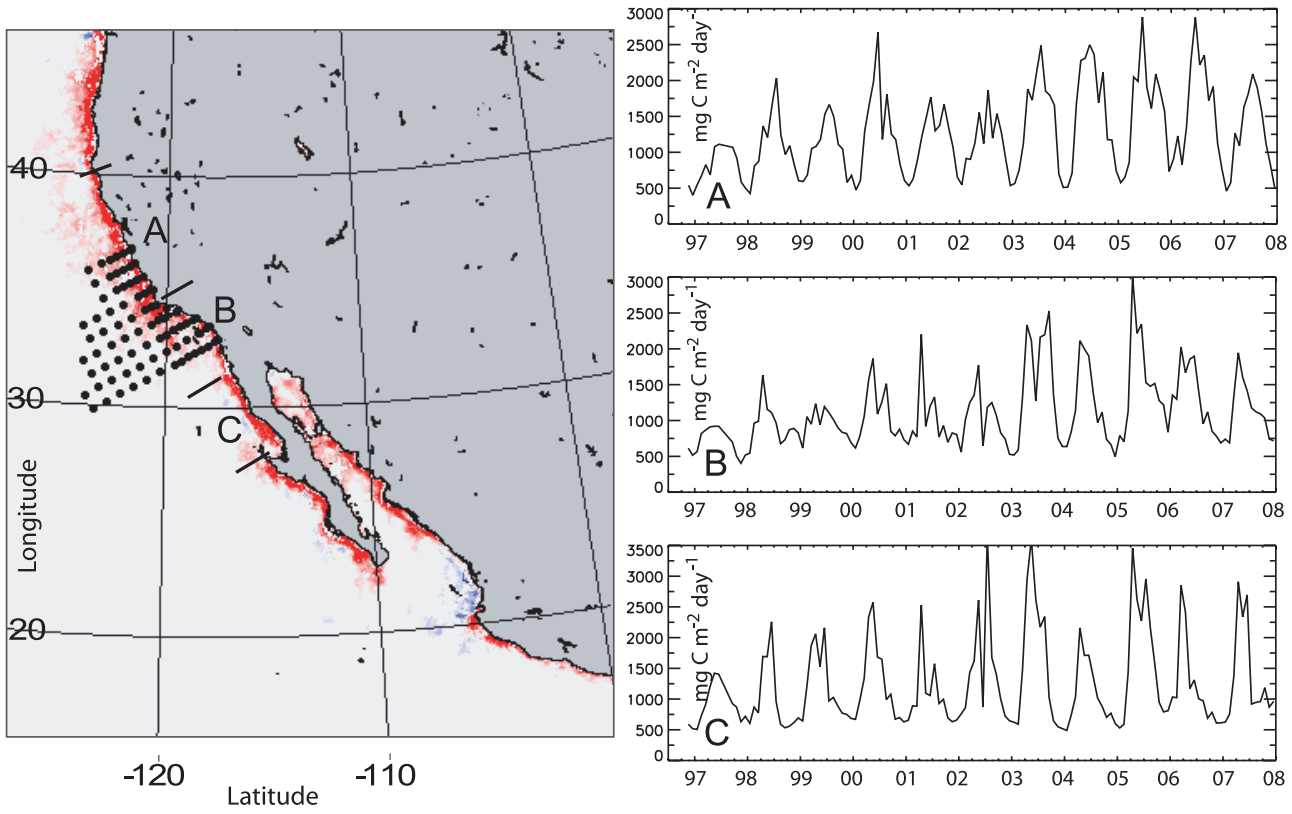

Figure 4. Map of the change in annual maximum primary production (calculated with the VGPM-CAL algorithm) during last 11 years (1997–2007). Red areas show significant increase detected by the Sen slope, a few blue areas have had significant decrease, and light gray areas have no detectable trend. The grid of the CalCOFI stations with in situ NPP measurements is shown as black filled circles. (right) Monthly time series of NPP in 50 km coastal strip off (left) Central California (area A), Southern California (area B), and Northern Baja California (area C).

conditions [*Kostadinov et al.*, 2007]. When applied to satellite data, the various NPP algorithms can yield differences up to 100%. Uncertainties in the input variables (especially for CbPM) make it difficult to compare the true merits of the algorithms (see *Friedrichs et al.* [2008] for more details). Much more work is needed to improve the NPP algorithms and the California Current is an ideal laboratory for this.

[22] A significant increase in the annual NPP maxima was detected along most of the coast of the California Current from 1997 to 2007. Related increases in annual maxima in Chl-a along the coast of the California Current as well as along the coasts of other major eastern boundary currents have been reported earlier [*Kahru and Mitchell*, 2008]. Given that Chl-a drives most of the response in these NPP models this increase in biomass will lead to corresponding increases in NPP. The increased blooms and production off the coast of Oregon are likely linked to the reported increase in hypoxia ("dead zones") [*Service*, 2004, 2007]. Some of the increase we observe can be attributed to the coincidence of the start of the 1997–2007 study period with the strong El Niño of 1997–1998 that suppressed Chl-a and NPP along the coasts [*Kahru and Mitchell*, 2002]. However, the increase in many areas is significant even after the 1997–1998 El Niño period. The timing of the annual maximum is also important: a good example was the delayed onset of upwelling in 2005 that resulted in large biomass and productivity decreases in the northern California Current [*Kudela et al.*, 2006; *Thomas and Brickley*, 2006].

[23] In the California Current increased upwelling is almost always associated with increased Chl-a, primary and secondary production [*Botsford et al.*, 2006; *Pennington et al.*, 2006; *Rykaczewski and Checkley*, 2008]. Therefore the observed increase in Chl-a and NPP along the coast might be most readily linked to increased upwelling. To test this hypothesis we used the wind-driven upwelling index (UI) based on estimates of offshore Ekman transport driven by geostrophic wind stress [*Schwing et al.*, 1996; Pacific Fisheries Environmental Laboratory, NOAA, unpublished data, 2008]. It appears, however, that UI does not show an increasing trend during 1997–2007 (Figure 5). On the contrary, weaker than average cumulative seasonal upwelling has been recorded during the second half of our study period and stronger than average cumulative seasonal upwelling during the first half [*Schwing et al.*, 2006]. This decrease in seasonal UI in 2004–2008 was observed in Central and Southern California while no trend in UI is evident in the Northern Baja region (Figure 5). In the 50 km coastal region of Central California annual NPP is positively correlated with SST (r^2 = 0.287) and negatively correlated with the annual maximum in UI (r^2 = 0.2739). While these correlations seem to be real, they are not statistically significant

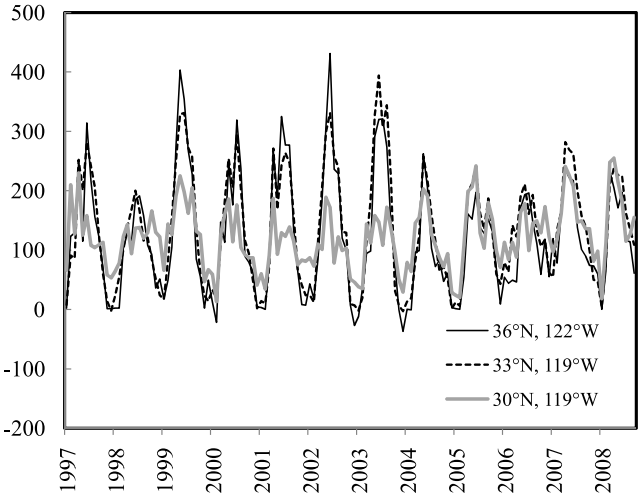

Figure 5. Upwelling index ($m^3\ s^{-1}\ 100\ m^{-1}$ coastline) at three locations corresponding to areas A, B, and C shown in Figure 4.

($p > 0.05$). However, in the Southern California and Northern Baja regions there is no correlation between NPP and either SST or UI. In summary, we detect an increasing trend of coastal NPP and Chl-a along most of the coast of the California Current and in Central California this trend is associated with decreased upwelling and increased SST while no correlation with SST and UI is evident in Southern California and Northern Baja regions. This suggests that the increased trend in Chl-a and NPP is not explained by seasonal upwelling intensity. Several authors have demonstrated from both empirical [*Palacios et al.*, 2004] and model data [*Di Lorenzo et al.*, 2005] that the California Current System exhibits long-term warming and increased stratification, which is predicted to reduce nutrient supplies and therefore NPP. Similarly, a global NPP analysis using VGPM suggests decreasing NPP due to surface warming and enhanced stratification [*Behrenfeld et al.*, 2006]. *Chhak and Di Lorenzo* [2007] also suggest that nutrient availability is modulated by the depth of upwelling in the California Current System, which in turn is regulated by the Pacific Decadal Oscillation (PDO). However, the PDO has been warm/positive during the time period presented here, which should result in lower nutrients and lower NPP. More recently, *Di Lorenzo et al.* [2008] have identified the North Pacific Gyre Oscillation (NPGO) as the dominant factor controlling nutrients in California Current (south of 38°N), and showed strong positive correlations between Chl-a and the NPGO. However, the observed increases in NPP occur during a period of both increasing and decreasing NPGO intensity.

[24] It is not clear what specific mechanism is driving the patterns of increased biomass in eastern boundary currents [*Kahru and Mitchell*, 2008] and increased NPP in the California Current. Previous authors have divided the California Current latitudinally and provide evidence for a combination (e.g., PDO, NPGO, ENSO) of forcing functions with varying effects at varying latitudinal bins [*Di Lorenzo et al.*, 2008; *Legaard and Thomas*, 2006; *Venegas et al.*, 2008]. We note that while latitudinal gradients certainly exist, driven by several identified mechanisms, the large-scale pattern is for increasing biomass and NPP within the entire coastal domain. None of these forcing mechanisms are directly correlated to the interannual trend identified in Chl-a and NPP for the full domain (data other than UI not shown). Assuming that the global offshore NPP will continue to decline in response to increased warming and stratification, the difference between the coastal ocean and offshore waters will almost certainly continue to increase. If this continues, eastern boundary current systems will become even more dominant in terms of NPP, and presumably carbon flux and trophic transfer.

[25] **Acknowledgments.** SeaWiFS, OCTS, and MODIS Aqua data were made available by the NASA Ocean Color Processing Group. Support by NASA Ocean Biogeochemistry and ECOHAB programs is acknowledged. This is a CCE LTER contribution 0077.

References

Abbott, M. R., and R. M. Letelier (1998), Decorrelation scales of chlorophyll as observed from bio-optical drifters in the California Current, *Deep Sea Res., Part II*, *45*, 1639–1667, doi:10.1016/S0967-0645(98)80011-8.

Balch, W. M., and C. F. Byrne (1994), Factors affecting the estimate of primary production from space, *J. Geophys. Res.*, *99*, 7555–7570, doi:10.1029/93JC03091.

Behrenfeld, M. J., and P. G. Falkowski (1997), Photosynthetic rates derived from satellite based chlorophyll concentration, *Limnol. Oceanogr.*, *42*, 1–20.

Behrenfeld, M. J., E. Boss, D. A. Siegel, and D. M. Shea (2005), Carbon-based ocean productivity and phytoplankton physiology from space, *Global Biogeochem. Cycles*, *19*, GB1006, doi:10.1029/2004GB002299.

Behrenfeld, M. J., R. O'Malley, D. Siegel, C. McClain, J. Sarmiento, G.Feldman, A. Milligan, P. Falkowski, R. Letelier, and E. Boss (2006), Climate-driven trends in contemporary ocean productivity, *Nature*, *444*, 752–755, doi:10.1038/nature05317.

Botsford, L. W., C. A. Lawrence, E. P. Dever, A. Hastings, and J. L. Largier (2006), Effects of variable upwelling on biological productivity on continental shelves in coastal upwelling systems, *Deep Sea Res., Part II*, *53*, 3116–3140, doi:10.1016/j.dsr2.2006.07.011.

Chavez, F. P., J. T. Pennington, C. G. Castro, J. P. Ryan, R. P. Michisaki, and B. Schilining (2002), Biological and chemical consequences of the 1997–1998 El Niño in central California waters, *Prog. Oceanogr.*, *54*, 205–232, doi:10.1016/S0079-6611(02)00050-2.

Chhak, K., and E. Di Lorenzo (2007), Decadal variations in the California Current upwelling cells, *Geophys. Res. Lett.*, *34*, L14604, doi:10.1029/2007GL030203.

Di Lorenzo, E., A. Miller, and N. Schneider (2005), The warming of the California Current System: Dynamics and ecosystem implications, *J. Phys. Oceanogr.*, *35*, 336–362, doi:10.1175/JPO-2690.1.

Di Lorenzo, E., et al. (2008), North Pacific Gyre Oscillation links ocean climate and ecosystem change, *Geophys. Res. Lett.*, *35*, L08607, doi:10.1029/2007GL032838.

Eppley, R. W. (1992), Chlorophyll, photosynthesis and new production in the Southern California Bight, *Prog. Oceanogr.*, *30*, 117–150, doi:10.1016/0079-6611(92)90010-W.

Eppley, R., E. Steward, M. Abbott, and U. Heyman (1985), Estimating ocean primary production from satellite chlorophyll: Introduction to regional differences and statistics for the southern California Bight, *J. Plankton Res.*, *7*, 57–70, doi:10.1093/plankt/7.1.57.

Field, C., M. Behrenfeld, J. Randerson, and P. Falkowski (1998), Primary production in the biosphere: Integrating terrestrial and oceanic components, *Science*, *281*, 237–241, doi:10.1126/science.281.5374.237.

Friedrichs, M. A. M., M.-E. Carr, R. T. Barber, M. Scardi, and the PPARR Team (2008), Assessing the uncertainties of model estimates of primary productivity in the tropical Pacific Ocean, *J. Mar. Syst.*, in press.

Gilbert, R. O. (1987), *Statistical Methods for Environmental Pollution Monitoring*, Van Nostrand Reinhold, New York.

Kahru, M., and B. G. Mitchell (1999), Empirical chlorophyll algorithm and preliminary SeaWiFS validation for the California Current, *Int. J. Remote Sens.*, *20*(17), 3423–3429, doi:10.1080/014311699211453.

Kahru, M., and B. G. Mitchell (2001), Seasonal and nonseasonal variability of satellite-derived chlorophyll and colored dissolved organic matter concentration in the California Current, *J. Geophys. Res.*, *106*, 2517–2529, doi:10.1029/1999JC000094.

Kahru, M., and B. G. Mitchell (2002), Influence of the El Niño–La Niña cycle on satellite-derived primary production in the California Current, *Geophys. Res. Lett.*, *29*(17), 1846, doi:10.1029/2002GL014963.

Kahru, M., and B. G. Mitchell (2008), Ocean color reveals increased blooms in various parts of the World, *Eos Trans. AGU*, *89*(18), 170, doi:10.1029/2008EO180002.

Kameda, T., and J. Ishizaka (2005), Size-fractionated primary production estimated by a two phytoplankton community model applicable to ocean color remote sensing, *J. Oceanogr.*, *61*, 663–672, doi:10.1007/s10872-005-0074-7.

Kostadinov, T. S., D. A. Siegel, S. Maritorena, and N. Guillocheau (2007), Ocean color observations and modeling for an optically complex site: Santa Barbara Channel, California, USA, *J. Geophys. Res.*, *112*, C07011, doi:10.1029/2006JC003526.

Kudela, R., and F. Chavez (2004), The impact of coastal runoff on ocean color during an El Niño year in Central California, *Deep Sea Res., Part II*, *51*, 1173–1185.

Kudela, R. M., W. P. Cochlan, T. D. Peterson, and C. G. Trick (2006), Impacts on phytoplankton biomass and productivity in the Pacific Northwest during the warm ocean conditions of 2005, *Geophys. Res. Lett.*, *33*, L22S06, doi:10.1029/2006GL026772.

Legaard, K. R., and A. C. Thomas (2006), Spatial patterns in seasonal and interannual variability of chlorophyll and sea surface temperature in the California Current, *J. Geophys. Res.*, *111*, C06032, doi:10.1029/2005JC003282.

Mantyla, A. W., E. L. Venrick, and T. L. Hayward (1995), Primary production and chlorophyll relationships, derived from ten years of CalCOFI measurements, *Calif. Coop. Ocean. Fish. Invest. Rep.*, *36*, 159–166.

Maritorena, S., D. A. Siegel, and A. R. Peterson (2002), Optimization of a semianalytical ocean color model for global-scale applications, *Appl. Opt.*, *41*, 2705–2714, doi:10.1364/AO.41.002705.

Marra, J., C. Ho, and C. Trees (2003), An alternative algorithm for the calculation of primary productivity from remote sensing data, *LDEO Tech. Rep. DEO-2003–DEO-1*, Lamont-Doherty Earth Observ. of Columbia Univ., New York, N. Y.

O'Reilly, J. E., S. Maritorena, B. G. Mitchell, D. A. Siegel, K. L. Carder, S. A. Garver, M. Kahru, and C. R. McClain (1998), Ocean color chlorophyll algorithms for SeaWiFS, *J. Geophys. Res.*, *103*, 24,937–24,953, doi:10.1029/98JC02160.

Palacios, D. P., S. J. Bograd, R. Mendelssohn, and F. B. Schwing (2004), Long-term and seasonal trends in stratification in the California Current, 1950–1993, *J. Geophys. Res.*, *109*, C10016, doi:10.1029/2004JC002380.

Pennington, J. T., K. L. Mahoney, V. S. Kuwahara, D. D. Kolber, R. Calienes, and F. P. Chavez (2006), Primary production in the eastern tropical Pacific: A review, *Prog. Oceanogr.*, *69*, 285–315, doi:10.1016/j.pocean.2006.03.012.

Rykaczewski, R. R., and D. M. Checkley (2008), Influence of ocean winds on the pelagic ecosystem in upwelling regions, *Proc. Natl. Acad. Sci. U. S. A.*, *105*, 1965–1970, doi:10.1073/pnas.0711777105.

Schwing, F. B., M. O'Farrell, J. M. Steger, and K. Baltz (1996), Coastal upwelling indices, west coast of North America, 1946–1995, *Tech. Memo. NOAA-TM-NMFS-SWFSC-231*, 144 pp., NOAA, La Jolla, Calif.

Schwing, F., N. Bond, S. Bograd, T. Mitchell, M. Alexander, and N. Mantua (2006), Delayed coastal upwelling along the U.S. West Coast in 2005: A historical perspective, *Geophys. Res. Lett.*, *33*, L22S01, doi:10.1029/2006GL026911.

Service, F. S. (2007), "Dead zone" reappears off Oregon coast, *ScienceNOW*, *31*, 3.

Service, R. F. (2004), New dead zone off Oregon coast hints at sea change in currents, *Science*, *305*, 1099, doi:10.1126/science.305.5687.1099.

Thomas, A., and P. Brickley (2006), Satellite measurements of chlorophyll distribution during spring 2005 in the California Current, *Geophys. Res. Lett.*, *33*, L22S05, doi:10.1029/2006GL026588.

Vander Woude, A. (2006), Coastal retentive embayments north and south of Point Reyes, California: Existence, timescales and carbon significance, Ph.D. dissertation, Univ. of California, Santa Cruz, Calif.

Venegas, R. M., P. T. Strub, E. Beier, R. Letelier, A. C. Thomas, T. Cowles, C. James, L. Soto-Mardones, and C. Cabrera (2008), Satellite-derived variability in chlorophyll, wind stress, sea surface height, and temperature in the northern California Current system, *J. Geophys. Res.*, *113*, C03015, doi:10.1029/2007JC004481.

Wheeler, P. A., A. Huyer, and J. Fleischbein (2003), Cold halocline, increased nutrients, and higher chlorophyll off Oregon in 2002, *Geophys. Res. Lett.*, *30*(15), 8021, doi:10.1029/2003GL017395.

M. Kahru and B. G. Mitchell, Scripps Institution of Oceanography, University of California, San Diego, La Jolla, CA 92121, USA. (mkahru@ucsd.edu)

R. Kudela, Ocean Sciences Department, University of California, Santa Cruz, CA 95064, USA.

M. Manzano-Sarabia, Centro de Investigaciones Biológicas del Noroeste, Mar Bermejo 195, La Paz, B.C.S. 23090, México.